MECHANICS OF RELAXING SiGe ISLANDS ON A VISCOUS GLASS

R. Huang[1], H. Yin[2], J. Liang[1], J.C. Sturm[2], K.D. Hobart[3], Z. Suo[1a]

[1] Mechanical and Aerospace Engineering Department and Princeton Materials Institute, Princeton University, Princeton, NJ 08544, USA.
[2]Center for Photonics and Optoelectronic Materials and Department of Electrical Engineering, Princeton University, Princeton, NJ 08544, USA.
[3]Naval Research Laboratory, Washington, DC 20375, USA.

This article is intended for the Proceedings of the
Workshop on Mechanics and Materials in the New Century, Xian, China, July 2001
To be published in a special issue of *Acta Mechanica Sinica*

a) Corresponding author. Email address: suo@princeton.edu

ABSTRACT: A process has been developed recently to fabricate a structure comprising, from top to bottom, a SiGe thin film, a glass layer, and a Si wafer. The SiGe film is a perfect crystal, and is under biaxial compression. Pattern the SiGe film into islands. On annealing, the glass flows and the islands relax. The resulting strain-free islands are used, as substrates, to grow epitaxial optoelectronic devices. This article describes a series of studies on the anneal process, combining experiment and theory. A small island relaxes by expansion, starting at the edges and diffusing to the center. A large island wrinkles before the expansion reaches the center. After some time, the wrinkles either disappear, or cause the island to fracture. We model the island as an elastic plate, and the glass layer as a viscous liquid. The strains in the islands are measured by x-ray diffraction and the Raman spectroscopy, and the wrinkle amplitudes by the atomic force microscope. The data are compared with the theoretical predictions. We determine the conditions under which the islands relax by expansion without significant wrinkling, and demonstrate that a cap layer suppresses wrinkles, relaxing a large island crack-free.

KEYWORDS: Semiconductor fabrication, stress relaxation, viscous flow, elastic plate, fracture

1 INTRODUCTION

Micro and nano fabrication processes provide a meeting ground between theory and experiment, and between science and technology [1,2]. An extensively studied example involves the growth of an epitaxial semiconductor film on a semiconductor substrate [3,4]. Other fabrication processes, such as wafer bonding, nanoimprint, electrodeposition, and self-assembly, all pose fascinating mechanics problems [5-14]. This article focuses on a specific process to fabricate SiGe on a silicon wafer. The two elements, Si and Ge, form solid solutions of any proportion. Ge has a lattice constant 4% larger than Si. By changing the composition, SiGe

solutions provide a range of lattice constants. On a relaxed SiGe, an epitaxial Si film is tensile and has a high electron mobility [15], and an epitaxial Ge film is compressive and has a high hole mobility [16]. The strained Si and Ge films are used for high-speed electronics [17]. Furthermore, Ge matches the lattice constant GaAs, a compound semiconductor for lasers [18]. Consequently, by relaxing SiGe (including pure Ge) on silicon, one can integrate high-performance electronic and optoelectronic devices on a single wafer.

One way to relax a SiGe layer on a silicon wafer is to allow dislocations to accommodate the lattice mismatch between SiGe and Si. Unfortunately, in addition to such geometrically necessary dislocations (i.e., the misfit dislocations), statistically stored dislocations (i.e., the threading dislocations) are abundant. The latter will thread into the epitaxial devices grown above the SiGe layer, impairing device performance. An improved approach is to grade the SiGe composition during growth [19,20]. The top SiGe layer grown this way has a lower threading dislocation density than a SiGe of the same composition grown directly on Si. The density, however, is still too high for some applications. Besides, this approach requires a thick total SiGe layer, which is a disadvantage.

Another way to relax SiGe is to use various "compliant substrates" [21-25]. Recently, Hobart and co-workers have studied the relaxation of SiGe islands transferred to a viscous borophosphorosilicate glass (BPSG) layer [26]. Following this initial work, we and others have studied this process with a combination of experiment and theory [27-35]. This article integrate these studies, provides evidence for wrinkle-induced fracture, and demonstrates an improved method to fabricate large, zero-defect, and strain-relaxed SiGe islands.

2 FABRICATION PROCESS

Figure 1 illustrates the fabrication process [26]. Grow an epitaxial SiGe film on a Si host wafer. The SiGe film has a larger lattice constant than Si, and is under biaxial compression. To avert dislocations, the SiGe film is below the critical thickness. Separately coat a BPSG layer on a Si handle wafer. Stack the two wafers by the wafer bonding method, with the SiGe facing the BPSG. Remove the Si host wafer, and then pattern the SiGe film into islands. Unless otherwise noted, the BPSG layer is 200 nm thick, and the SiGe film is 30 nm thick. The experiment uses $Si_{0.7}Ge_{0.3}$, with lattice constant 1.2% larger than Si, patterned into square islands of various sizes, L = 10μm – 500μm. Before anneal, the SiGe islands are under the 1.2% biaxial compressive strain, because the island size is much larger than the island thickness, and the BPSG is solid at room temperature. On annealing above the glass transition temperature, the glass flows, and the islands relax elastically. The process involves no dislocations and, in principle, produces zero-defect, relaxed SiGe islands. The resulting strain-free islands can be used as substrates to grow epitaxial optoelectronic devices. For this purpose, large islands are desired.

Islands of various sizes are annealed above the glass transition temperature of BPSG [35]. Small islands (L < 30 μm) expand, but large islands wrinkle. After a long anneal, the wrinkles disappear for mid-sized islands (30μm < L < 80μm), but cause fracture for large islands. Figure 2 shows part of a 100μm island annealed for 90 minutes at 790°C. At the corner, the island expands in both inplane directions, and remains flat. At each edge, the island expands in one direction, and wrinkles in the other. At the center, and island wrinkles in a complicated way. Figure 3 shows a 200μm island annealed for 90 minutes at 790°C. In addition to wrinkles, channel cracks form in the island, probably initiated from the island edges. It is the wrinkle-induced fracture that limits the size of the islands to be relaxed.

3 GENERAL THEORY

Figure 4 illustrates the model. The SiGe island is taken to be elastic, the BPSG viscous, and the Si wafer rigid. Maintain the continuity of velocities and tractions at the SiGe-BPSG interface, and zero velocity at the BPSG-Si interface. The island is flat and under biaxial stresses in the initial state, which serves as the reference state. On annealing, the island expands and wrinkles. Let u_1 and u_2 be the inplane displacements, and w be the deflection, all set to zero in the initial state. On the SiGe-BPSG interface, let q be the normal traction, and T_1 and T_2 be the shear tractions. The elasticity of the SiGe island relates the tractions on the interface to the displacement field. The viscous flow of the BPSG layer relates the velocity field to the tractions. The combination relates the velocity field to the displacement field, evolving the system. The following prescribes the theory.

To describe both expansion and wrinkling, we model the elastic SiGe island using the von Karman plate theory [36,37]. The membrane strains have three contributions:

$$\varepsilon_{\alpha\beta} = -\varepsilon_0 \delta_{\alpha\beta} + \frac{1}{2}\left(\frac{\partial u_\alpha}{\partial x_\beta} + \frac{\partial u_\beta}{\partial x_\alpha}\right) + \frac{1}{2}\frac{\partial w}{\partial x_\alpha}\frac{\partial w}{\partial x_\beta}. \tag{1}$$

The first comes from the initial biaxial compressive strain, ε_0 being the magnitude; the second from the gradients of the inplane displacements; and the third from the large deflection. The Greek subscript takes values 1 and 2. Hooke's law relates the membrane forces $N_{\alpha\beta}$ to the membrane strains $\varepsilon_{\alpha\beta}$:

$$N_{\alpha\beta} = Eh\left[\frac{1}{1+\nu}\varepsilon_{\alpha\beta} + \frac{\nu}{1-\nu^2}\varepsilon_{\gamma\gamma}\delta_{\alpha\beta}\right], \tag{2}$$

where E is Young's modulus, ν Poisson's ratio, and h thickness of the island. A repeated Greek subscript implies summation over 1 and 2. The inplane force balance of a plate element requires that

$$T_\alpha = \frac{\partial N_{\alpha\beta}}{\partial x_\beta}. \tag{3}$$

The out-of-plane force balance and the moment balance of a plate element requires that

$$q = -\frac{Eh^3}{12(1-\nu^2)}\frac{\partial^4 w}{\partial x_\alpha \partial x_\alpha \partial x_\beta \partial x_\beta} + N_{\alpha\beta}\frac{\partial^2 w}{\partial x_\alpha \partial x_\beta} + T_\alpha \frac{\partial w}{\partial x_\alpha}. \tag{4}$$

In essence, the plate theory provides an algorithm to calculate the tractions on the interface, T_1, T_2, q, in terms of the displacement field of the island, u_1, u_2, w.

We model the BPSG layer above the glass transition temperature as an incompressible viscous liquid, adopt the Stokes creep theory [38] in this section, and describe specialized models in the subsequent sections. The stress field in the glass layer, σ_{ij}, is in equilibrium, so that

$$\frac{\partial \sigma_{ij}}{\partial x_j} = 0. \tag{5}$$

The Latin indices take values 1, 2 and 3, and a repeated Latin index implies summation over 1, 2 and 3. The stresses relate to the velocities V_i as

$$\sigma_{ij} = -p\delta_{ij} + \eta\left(\frac{\partial V_i}{\partial x_j} + \frac{\partial V_j}{\partial x_i}\right), \tag{6}$$

where p is the pressure and η the viscosity of the glass. Incompressibility requires that

$$\frac{\partial V_i}{\partial x_i} = 0. \tag{7}$$

The velocity field at the BPSG-Si interface vanishes, and the tractions on the BPSG-SiGe interface are T_1, T_2, q. Equations (5)-(7), together with the boundary conditions, define a moving

boundary value problem. In essence, the fluid mechanics of the BPSG layer provides an algorithm to calculate the velocity field in terms of the tractions on the BPSG-SiGe interface.

The coupled solid-liquid problem is nonlinear, with solutions of several kinds, corresponding to the growing wrinkles, the equilibrium wrinkles, the flat strained blanket film, and the relaxed island. The following sections reduce the general theory to simpler models, and compare the solutions to experiments.

4 ISLAND EXPANSION

The problem is greatly simplified if we focus on island expansion, neglecting the wrinkles, and assuming the shear stress in the BPSG layer to be uniform across its thickness [27-29]. The resulting approximation, known as the shear lag model, dates back to the studies of tectonic plate drift [39-41].

To see how the shear lag model describes island expansion, here we examine the relaxation in the x_1 direction. The only nonzero displacement component is $u_1(x_1,t)$. From (1), the membrane strains are

$$\varepsilon_{11} = -\varepsilon_0 + \frac{\partial u_1}{\partial x_1},\ \varepsilon_{22} = -\varepsilon_0,\ \varepsilon_{12} = 0\,. \tag{8}$$

Hooke's law (2) gives the membrane force component in the x_1 direction,

$$N_{11} = -\frac{Eh}{1-\nu}\varepsilon_0 + \frac{Eh}{1-\nu^2}\frac{\partial u_1}{\partial x_1}\,. \tag{9}$$

The first term is the initial compressive membrane force, and the second term accounts for expansion. The inplane force balance in the x_1 direction, of a SiGe film element, relates the shear traction on the interface, T_1, to the divergence of the membrane force, namely,

$$\frac{\partial N_{11}}{\partial x_1} = T_1. \tag{10}$$

Assume that the shear stress in the BPSG is uniform across its thickness, so is the shear strain-rate, approximated by $(\partial u_1 / \partial t)/H$, where H is the thickness of the BPSG. The shear stress is linear in the shear strain-rate:

$$T_1 = \frac{\eta}{H}\frac{\partial u_1}{\partial t}. \tag{11}$$

A combination of (9)-(11) leads to

$$\frac{\partial u_1}{\partial t} = \frac{EhH}{(1-\nu^2)\eta}\frac{\partial^2 u_1}{\partial x_1^2}. \tag{12}$$

Equation (12) has the form of the diffusion equation, with $EhH/(1-\nu^2)\eta$ being the effective diffusivity. Now consider the expansion of an island of length L. At $t = 0$, the membrane force N_{11} vanishes at the two edges, and equals $-Eh\varepsilon_0/(1-\nu)$ inside the island. On annealing, the expansion starts at the island edges, and diffuses to the island center. As $t \to \infty$, the membrane force $N_{11} \to 0$ in the entire island.

The solution of this classical initial-boundary value problem takes the form of an infinite series, the slowest decaying term being proportional to $\exp(-t/t_E)$, with

$$t_E = \frac{1-\nu^2}{\pi^2}\frac{L^2}{Hh}\frac{\eta}{E}. \tag{13}$$

We take t_E as the time scale for island expansion. Equation (13) is also obtained by dimensional considerations, except for the factor π^2. The expansion time t_E depends on the dimensionless ratio L^2/Hh, and the ratio η/E that has the dimension of time. A large island takes a long time to relax.

The shear lag model has also been formulated in two dimensions [41], and solved numerically for the expansion of a square island [29]. Figure 5 plots the strain scaled by the initial mismatch strain, against the time scaled by the square of the island size [35]. With such scaling, the shear lag model predicts one single curve in each plot for all island sizes. The experimental data for islands of various sizes fall on the same curve, confirming this scaling law. We use x-ray diffraction to measure the average strain in the island (Fig. 5a), and Raman spectroscopy to measure the strain at the island center (Fig. 5b). Comparing the experimental data and the numerical solution, we determine the viscosity of BPSG: η = 12.2 GPa s at 790°C, and η = 52.5 GPa s at 750°C.

5 GROWING WRINKLES

We next consider wrinkles in a blanket SiGe film (i.e., an infinite island). When a flat blanket film is under a uniform biaxial compression, generating no tractions on the SiGe-BPSG interface, the BPSG does not creep. This equilibrium state is a trivial solution to the problem posed in Section 3. The equilibrium state, however, is unstable. The elastic energy stored in the SiGe film reduces when the film wrinkles. To describe the salient features of the wrinkle dynamics, here we give a simplified analysis, assuming that the BPSG layer is so thick that its thickness does not enter the consideration. The analysis follows those in [42,30]. More comprehensive analyses are given in [31-33].

Perturb the film with a sinusoidal deflection

$$w(x_1,t) = A(t)\sin\left(\frac{2\pi x_1}{\lambda}\right). \tag{14}$$

where $A(t)$ is the time-dependent winkle amplitude, and λ the wrinkle wavelength. The analysis assumes that the amplitude A is small, and keeps only the terms linear in A.

To the first order in A, the membrane force is unperturbed, given by its initial value $N_{11} = -Eh\varepsilon_0/(1-\nu)$, and the shear traction T_1 vanishes. Equation (4) becomes

$$q = \left[-\frac{Eh^3}{12(1-\nu^2)}\left(\frac{2\pi}{\lambda}\right)^4 + \frac{Eh\varepsilon_0}{1-\nu}\left(\frac{2\pi}{\lambda}\right)^2 \right] A(t)\sin\left(\frac{2\pi x_1}{\lambda}\right). \tag{15}$$

Subject to this traction on the interface, the BPSG creeps, and its velocity field is determined by solving the creep problem posed in Section 3. The velocity of the surface, $\partial w/\partial t$, is proportional to a representative strain rate, q/η, and to a length scale, λ, giving

$$\frac{\partial w}{\partial t} = \frac{\lambda q}{4\pi\eta}. \tag{16}$$

The factor 4π is determined by solving the boundary value problem.

Inserting (14) and (15) into (16) yields a differential equation $dA/dt = sA$, with

$$s = \frac{E}{24\eta(1-\nu^2)}\left[-\left(\frac{2\pi h}{\lambda}\right)^3 + 12(1+\nu)\varepsilon_0\left(\frac{2\pi h}{\lambda}\right) \right]. \tag{17}$$

The solution to this differential equation is $A(t) = A_0\exp(st)$, where A_0 is the initial wrinkle amplitude. The parameter s governs the rate of change in the winkle amplitude. When a flat film winkles, the bending increases the energy stored in the film, but the inplane compression does work to decrease the energy. The two actions correspond to the two terms in the bracket of (17).

Figure 6 sketches s as a function of the wavelength. The value of s vanishes at the critical wavelength

$$\lambda_c = \frac{\pi h}{\sqrt{3(1+\nu)\varepsilon_0}}, \tag{18}$$

which reproduces the Euler buckling condition. When $\lambda < \lambda_c$, the bending costs too much energy, $s < 0$, and the winkles decay over time. When $\lambda > \lambda_c$, the work done by the inplane

compression prevails, $s > 0$, and the winkles amplify over time. When $\lambda \to \infty$, creep over the long distance takes a long time, so that $s \to 0$.

The value of s reaches a maximum value

$$s_m = \frac{2\sqrt{1+\nu}\,\varepsilon_0^{3/2}}{3(1-\nu)}\frac{E}{\eta} \tag{19}$$

at the wavelength

$$\lambda_m = \frac{\pi h}{\sqrt{(1+\nu)\varepsilon_0}}. \tag{20}$$

Wrinkles of this wavelength amplify fastest. Using $\nu = 0.3$, $\varepsilon_0 = 0.012$, and h = 30 nm, Equation (20) gives $\lambda_m = 0.75$ μm. The wavelength observed experimentally is about 1μm (Fig. 2). The agreement is reasonable.

The fastest amplifying winkles obey $A(t) = A_0 \exp(s_m t)$. The time for the wrinkles to amplify from the initial amplitude A_0 to amplitude A is

$$t_W = \frac{3(1-\nu)}{2\sqrt{1+\nu}\,\varepsilon_0^{3/2}} \ln\left(\frac{A}{A_0}\right)\frac{\eta}{E}. \tag{21}$$

We measure the surface roughness as a function of annealing time by using the atomic force microscope. Figure 7 plots the experimental data for 30 nm and 60 nm thick SiGe films [35]. The predictions of the linear perturbation analysis correspond to the straight lines in Fig. 7. We use the viscosity extracted in the previous section from inplane expansion of small islands, and use the initial amplitude A_0 as the single fitting parameter. The agreement between theory and experiment is excellent for the initial stage of wrinkling.

6 EQUILIBRIUM WRINKLES

Figure 7 shows that, for the 30nm film, the wrinkle amplitude saturates after about 1 hour anneal. That is, the wrinkles attain an equilibrium state, the BPSG stops creeping, and the tractions on the interface vanish. Such an equilibrium state is similar to the post-buckling state of a column under an axial force. However, there is an important difference. For the column, the post-buckling state is maintained by the prescribed axial displacement at the two ends of the column. For the blanket film, no displacement is prescribed, so that the equilibrium wrinkles are unstable, and can reduce energy further by evolving into wrinkles of longer wavelengths. The wrinkles, however, coarsen slowly because of the viscosity of the BPSG layer. Consequently, the saturated wrinkles of any wavelength are in a kinetically constrained equilibrium state.

The mechanical property of the underlayer affects the wrinkles in the compressed film. This fact is brought to attention recently in the development of low dielectric constant polymers for interconnect structures [43]. These authors coat a silicon wafer with a polymer layer, and then deposit a SiN thin film on the polymer, with the SiN film under a compressive residual stress. The SiN film remains flat on annealing below the glass transition temperature T_g of the polymer underlayer, but wrinkles on annealing above the T_g of the underlayer. In both cases, wrinkles would lower the elastic energy stored in the SiN film. Below T_g, the polymer underlayer is elastic, and the SiN film remains flat, because the wrinkles would add too much elastic energy to the underlayer. Above T_g, the polymer underlayer creeps, and the SiN film wrinkles, the elastic energy in the underlayer decaying over a long time. Of course, if the polymer underlayer below T_g has a very low elastic modulus, the stressed film will form wrinkles, which only add a small amount of elastic energy in the underlayer. Such wrinkles are in a stable equilibrium state, and will not coarsen over time. This behavior is studied in a

compressed gold film on a rubber [44]. The behaviors of the wrinkles, easily observable in experiments, provide a means to determine mechanical properties of the underlayer.

We now analyze the equilibrium wrinkles, following a similar analysis for buckle-delamination of thin films [45]. Consider a film that wrinkles in the x_1 direction, with nonzero displacements $w(x_1)$ and $u_1(x_1)$. Specializing the general theory in Section 3, we find that the membrane force relates to the displacements as

$$N_{11} = -\frac{Eh}{1-\nu}\varepsilon_0 + \frac{Eh}{1-\nu^2}\left[\frac{du_1}{dx_1} + \frac{1}{2}\left(\frac{dw}{dx_1}\right)^2\right]. \tag{22}$$

In equilibrium, the tractions on the interface, q and T_1, vanish, so that the moment balance equation (4) reduces to

$$\frac{Eh^3}{12(1-\nu^2)}\frac{d^4w}{dx_1^4} = N_{11}\frac{d^2w}{dx_1^2}. \tag{23}$$

When the shear traction T_1 vanishes, inplane force equilibrium requires that the membrane force N_{11} be a constant in the film. Consequently, the ordinary differential equation (23) has constant coefficients. The nontrivial solution $w(x_1)$ is of the sinusoidal form of (14). Substituting (14) into (23), we obtain that

$$N_{11} = -\left(\frac{\lambda_c}{\lambda}\right)^2 \frac{Eh\varepsilon_0}{1-\nu}, \tag{24}$$

where λ_c is the critical wavelength given by (18). The longer the wavelength, the lower the amplitude of the membrane force.

Substituting (14) and (24) into (22), we find the equilibrium wrinkle amplitude

$$A_{eq} = \frac{h}{\sqrt{3}}\sqrt{\left(\frac{\lambda}{\lambda_c}\right)^2 - 1}, \tag{25}$$

and the inplane displacement field

$$u_1(x_1) = -\frac{\pi}{4\lambda} A_{eq}^2 \sin\left(\frac{4\pi x_1}{\lambda}\right). \tag{26}$$

In the equilibrium winkles, the inplane displacement undulates with the wavelength half that of the deflection.

For any wavelength $\lambda > \lambda_c$, a nontrivial equilibrium state exists. Consequently, infinitely many such equilibrium states exist for a blanket film. On the other hand, the viscous layer controls the wrinkling rate. The fastest growing mode, of wavelength λ_m, prevails at the initial stage. As the wrinkles approach the equilibrium state of wavelength λ_m, creep slows down, and the film is kinetically constrained near this equilibrium state, making such state observable in experiment. Comparing (18) and (20), we note that $\lambda_m / \lambda_c = \sqrt{3}$. Consequently, the winkles of wavelength λ_m have equilibrium amplitude $A_{eq} = \sqrt{2/3}h$. This agrees reasonably well with the experiment (Fig. 7).

We next consider fracture induced by the wrinkles. At the crest of a wrinkle, the stress is the sum of that due to the membrane force, and that due to the bending moment, namely,

$$\sigma = \frac{N_{11}}{h} - \frac{Eh}{2(1-\nu^2)} \frac{d^2 w}{dx_1^2}. \tag{27}$$

For equilibrium wrinkles of wavelength λ, this stress is

$$\sigma_{eq} = \frac{E\varepsilon_0}{1-\nu}\left(\frac{\lambda_c}{\lambda}\right)^2 \left[2\sqrt{3}\left(\left(\frac{\lambda}{\lambda_c}\right)^2 - 1\right)^{1/2} - 1 \right]. \tag{28}$$

The stress becomes tensile when $\lambda / \lambda_c > \sqrt{13/12}$. For wrinkles of the wavelength λ_m, Equation (28) simplifies to $\sigma_{eq} \approx 1.3\varepsilon_0 E/(1-\nu)$. Using representative values, $\varepsilon_0 = 0.012$, $E = 150\text{GPa}$ and $\nu = 0.3$, we find that $\sigma_{eq} = 3.3\text{GPa}$. The toughness of SiGe is about $K_c \approx 1\text{MPa}\sqrt{\text{m}}$. The

critical flaw size is $a_c \approx \left(K_c / \sigma_{eq}\right)^2 / \pi \approx 29\,\text{nm}$, which is close to the thickness of the SiGe films. Flaws of this size are expected at the edges of the islands.

7 THE RACE BETWEEN EXPANSION AND WRINKLING

The shear lag model describes the island expansion, neglecting wrinkling. The two wrinkling models analyze a blanket film, neglecting island expansion. In reality, an island expands and wrinkles concomitantly. We adapt the Reynolds lubrication theory [46] to model the creep in the BPSG layer, taking into account of the boundary conditions imposed by the elastic island. The velocity field relates to the tractions as [32]

$$\frac{\partial u_\alpha}{\partial t} = \frac{H^2}{2\eta}\frac{\partial q}{\partial x_\alpha} + \frac{H}{\eta}T_\alpha, \tag{29}$$

$$\frac{\partial w}{\partial t} = \frac{\partial}{\partial x_\alpha}\left(-\frac{H^3}{3\eta}\frac{\partial q}{\partial x_\alpha} - \frac{H^2}{2\eta}T_\alpha\right), \tag{30}$$

where $H = H_0 + w(x_1, x_2, t)$, with H_0 being the average thickness of the glass layer. The lubrication theory describes the three dimensional flow in the glass layer with partial differential equations in two dimensions, and is justified when the thickness of the glass layer is small compared to the wrinkle wavelength. The shear lag model is a special case of the lubrication theory, as evident by comparing (11) and (29).

Recall that the tractions relate to the displacement field by the elastic plate theory, which, together with (29) and (30), evolves the displacement field. Figure 8 shows the computed wrinkle amplitude at the island center as a function of time [34]. Included are islands of three sizes, L = 15μm, 30μm, 60μm. The dashed lines are the results of linear perturbation (LP) and constrained equilibrium (CE). The wrinkle amplitude of every island grows exponentially

initially, as predicted by the linear perturbation analysis. For the island of size L = 15μm, the expansion reaches the island center before the wrinkle amplitude attains CE and, subsequently, the wrinkle amplitude decays. For a larger island (L = 30μm), the wrinkle amplitude attains CE, stays there for a while, and then decays when expansion arrives. For a still larger island (L = 60μm), the wrinkle amplitude stays at CE for a longer time, but eventually will also decay when expansion arrives.

Experimental observations have indicated that, everything else being equal, there exists a critical island size, L_c: small islands expand, and large islands wrinkle and fracture. What determines the critical island size? Clearly the wrinkle wavelength does *not* set the critical island size. As shown in Fig. 2, the wrinkle wavelength is about 1 μm, and our experiment shows that the critical island size is somewhere between 30μm and 80μm. It is the race between expansion and wrinkling that determines the critical island size. The expansion time Eq. (13) depends on the film size L, but the wrinkling time Eq. (21) does not. For a small island, expansion reaches the island center in a short time, before the wrinkles grow much. For a large island, expansion takes a long time to reach the island center, so that the wrinkles have a plenty of time to amplify to cause fracture. The critical island size is estimated by setting $t_E = t_W$, giving

$$L_c = \frac{\pi}{\left[(1+\nu)\varepsilon_0\right]^{3/4}}\sqrt{\frac{3Hh}{2}\ln\left(\frac{A_c}{A_0}\right)}\ , \tag{31}$$

where A_c is a critical wrinkle amplitude, at which the tensile stress at the wrinkle crests may cause fracture. Although the value A_c depends on the flaw size in the film, the critical island size L_c only weakly depends on A_c. An estimate from Eq. (31) gives $L_c \approx 20\mu$m, which agrees with the experimental observation reasonably well. The critical island size is independent of the glass viscosity η, because reducing the viscosity accelerates expansion and wrinkling proportionally.

8 WRINKLE SUPPRESSION BY CAP LAYER

Figure 9 illustrates a process that can fabricate islands larger than the critical island size described above. Before annealing, a strain-free cap layer is deposited on the strained SiGe island. After first annealing, the cap-SiGe bilayer reaches the force balance, tensile in the cap layer, and compressive in the SiGe island. The compressive stress in SiGe is reduced from the initial state. Then, the cap layer is removed and the remaining SiGe film is annealed again to achieve full relaxation. During the first anneal, since the effective thickness of the island is larger and the effective compressive stress is smaller, the critical island size is larger than the original critical island size for SiGe islands without the cap layer. In the second anneal, since the compressive strain in SiGe has been partially relaxed, the critical island size is also larger.

Figure 10 shows the micrographs of several annealed islands (L = 200μm and 500μm). Without the cap, the islands of both sizes fracture. With a 19nm thick cap, the 200μm island is crack-free, but the 500μm island still factures although the improvement is obvious. A thicker cap is required to relax the 500μm islands crack-free. For very large islands, multiple etching and annealing steps may be required.

9 CONCLUDING REMARKS

This paper describes a series of studies on a compressed SiGe island on a glass layer. Annealing is in effect a race between two processes: expansion and wrinkling. For a small island, expansion prevails, and the island relaxes to the stress-free state. For a large island, winkling prevails, and the island develops tensile stress and fractures. We model the island as an elastic plate, and the glass layer as a viscous liquid. The theory is compared with the experiment

at various points. Using a cap layer, we can relax large islands and avert wrinkle fracture. The behaviors of thin film wrinkles, so easily observable in experiments, provide a means to measure mechanical properties of the underlayer. For example, our experimental data of the wrinkle amplitude as a function of time provide a reliable means to determine the viscosity of BPSG.

ACKNOWLEDGEMENTS

This work is supported by NSF (CMS-9820713), DARPA (N66001-00-1-8957), ARO (DAA655-98-1-0270), and New Jersey Science and Technology Commission.

REFERENCES

1 Freund LB. The mechanics of electronic materials. *Int. J. Solids Structures*, 2000, 37: 185~196

2 Suo Z. Evolving material structures of small feature sizes. *Int. J. Solids Structures*, 2000, 37: 367~378

3 Gao H, Nix WD. Surface roughening of heteroepitaxial thin films. *Ann. Rev. Mater. Sci.* 1999, 29: 173~209

4 Bruner K. Si/Ge nanostructures. *Rep. Porg. Phys.*, 2002, 65: 27~72

5 Tong QY, Gosele U. Semiconductor Wafer Bonding: Science and Technology, Wiley, New York, 1998

6 Yu H, Suo Z. A model of wafer bonding by elastic accommodation. *J. Mech. Phys. Solids*, 1998, 46: 829~844

7 Li M, Wang J, Zhuang L, Chou SY. Fabrication of circular optical structures with a 20 nm minimum feature size using nanoimprint lithography. *Appl. Phys. Lett.*, 2000, 76:673~675

8 Kim C, Burrows PE, Forrest SR. Micropatterning of organic electronic devices by cold welding. *Science*, 2000, 288:831~833

9 Josell D, Wheeler D, Huber WH, Moffat TP. Superconformal electrodeposition in submicron features. *Phys. Rev. Lett.*, 2001, 87:016102

10 Haataja M, Srolovitz DJ. Morphological instability and additive-induced stabilization in electrodeposition. Submitted for publication.

11 Liang J, Suo Z. Stable island arrays by height-constrained Stranski-Krastanov growth. *Applied Physics Letters,* 2001, 79:3251~3252

12 Suo Z, Lu W. Forces that drive self-assembly on solid surfaces. *Journal of Nanoparticles Research*, 2000, 2:333~344

13 Chou SY, Zhuang L, Gao L. Lithographically induced self-construction of polymer microstructures for resistless patterning. *Appl. Phys. Lett.*, 1999, 75: 1004~1006

14 Erlebacher J, Aziz MJ, Chason E, Sinclair MB, Floro JA. Nonlinear amplitude evolution during spontaneous patterning of ion-bombarded Si(001). *J. Vac. Sci. Techno.* A, 2000, 18: 115~120

15 Ismail K, Arafa M, Saenger KL, Chu JO, Meyerson BS. Extremely high electron mobility in Si/SiGe modulation-doped heterostructures. *Appl. Phys. Lett.*, 1995, 66: 1077~1079

16 Xie YH, Monroe D, Fitzgerald EA, Silverman PJ, Thiel FA, Watson GP. Very high mobility two-dimensional hole gas in Si/Ge_xSi_{1-x}/Ge structures grown by molecular beam epitaxy. *Appl. Phys. Lett.*, 1993, 63: 2263~2265

17 Mooney PM, Chu JO. SiGe technology: heteroepitaxy and high-speed microelectronics. *Annu. Rev. Mater. Sci.*, 2000, 30: 335~3625

18 Fitzgerald EA, Xie YH, Monroe D, Silverman PJ, Kuo JM, Kortan AR, Thiel FA, Weir BE. Relaxed Ge_xSi_{1-x} structures for III–V integration with Si and high mobility two-dimensional electron gases in Si. *J. Vac. Sci. Technol. B.*, 1992, 10: 1807~1819

19 Fitzgerald EA, Xie YH, Green ML, Brasen D, Kortan AR, Michel J, Mii YJ, Weir BE. Totally relaxed Ge_xSi_{1-x} layers with low threading dislocation densities grown on Si substrates. *Appl. Phys. Lett.*, 1991, 59: 811~813

20 Fitzgerald EA. GeSi/Si nanostrcutures. *Annu. Rev. Mater. Sci.*, 1995, 25: 417~45

21 Lo YH. New approach to grow pseudomorphic structures over the critical thickness. *Appl. Phys. Lett.*, 1991, 59: 2311~2313

22 Powell AR, Iyer SS, LeGoues FK. New approach to the growth of low dislocation relaxed SiGe material. *Appl. Phys. Lett.*, 1994, 64: 1856~1858

23 Yang Z, Alperin J, Wang WI, Iyer SS, Kuan TS, Semendy F. *In situ* relaxed $Si_{1-x}Ge_x$ epitaxial layers with low threading dislocation densities grown on compliant Si-on-insulator substrates. *J. Vac. Sci. Technol. B.*, 1998, 16: 1489~1491

24 Huang FY, Chu MA, Tanner MO, Wang KL, U'Ren GD, Goorsky MS. High-quality strain-relaxed SiGe alloy grown on implanted silicon-on-insulator substrate. *Appl. Phys. Lett.*, 2000, 76: 2680~2682

25 Vanhollebeke K, Moerman I, Van Daele P, Demeester P. Compliant substrate technology: investigation of mismatched materials for opto-electronic applications. *Progress in Crystal Growth and Characterization of Materials*, 2000: 1~55

26 Hobart KD, Kub FJ, Fatemi M, Twigg ME, Thompson PE, Kuan TS, Inoki CK. Compliant substrates: a comparative study of the relaxation mechanisms of strained films bonded to high and low viscosity oxides. J. Electronic Materials, 2000, 29: 897~900

27 Freund LB, Nix WD. (Unpublished)

28 Movan PD, Kuech TF. Kinetics of strain relaxation in semiconductor films grown on borosilicate glass-bonded substrates. *J. Electronic Materials*, 2001, 30:802~806

29 Huang R, Yin H, Liang J, Hobart KD, Sturm JC, Suo Z. Relaxation of a strained elastic film on a viscous layer. *Mater. Res. Soc. Symp. Proc.*, 2001, 695: 115~120

30 Sridhar N, Srolovitz DJ, Suo Z. Kinetics of buckling of a compressed film on a viscous substrate. *Appl. Phys. Lett.*, 2001, 78: 2482~2484

31 Huang R, Suo Z. Instability of a compressed elastic film on a viscous layer. *Int. J. Solids Struct.*, 2002, 39: 1791~1802

32 Huang R, Suo Z. Wrinkling of a compressed elastic film on a viscous layer. *J. Appl. Phys.*, 2002, 91: 1135~1142

33 Sridhar N, Srolovitz DJ, Cox BN. Buckling and post-buckling kinetics of compressed thin films on viscous substrates. *Acta Mater.*, 2002, 50:2547~2557

34 Liang J, Huang R, Yin H, Sturm JC, Hobart KD, Suo Z. Relaxation of compressed elastic islands on a viscous layer. *Acta Materialia*, 2002, 50:2933~2944

35 Yin H, Huang R, Hobart KD, Suo Z, Kuan TS, Inoki CK, Shieh SR, Duffy TS, Kub FJ, Sturm JC. Strain relaxation of SiGe islands on compliant oxide. *J. Appl. Phys.*, 2002, 91: 9716~9722

36 Timoshenko S, Woinowsky-Krieger S. Theory of Plates and Shells, 2nd edition. McGraw-Hill, Inc., New York, 1987

37 Landau D, Lifshitz EM. Theory of Elasticity. Pergamon Press, London, 1959

38 Bachelor GK. An Introduction to Fluid Dyanmics. Cambridge University Press, Cambridge, 1967

39 Elsasser WM. Convection and stress propagation in the upper mantle. In *The Application of Modern Physics to the Earth and Planetary Interiors*, edited by Runcorn WK. Weily, New York, 1969: 223~246

40 Bott MH, Dean DS. Stress diffusion from plate boundaries. *Nature*, 1973, 243: 339~341

41 Lehner FK, Li VC, Rice JR. Stress diffusion along rupturing plate boundaries. *J. Geophysical Research*, 1981, 86: 6155~6169

42 Suo Z. Wrinkling of the oxide scale on an aluminum-containing alloy at high temperatures. *J. Mech. Phys. Solids*, 1995, 43:829~846

43 Martin SJ, Godschalx JP, Mills ME, Shaffer EO, Townsend PH. Development of a low-dielectric-constant polymer for the fabrication of integrated circuit interconnect. *Advanced Materials*, 2000, 12:1769~1778

44 Bowden N, Brittan S, Evans AG, Hutchinson JW, Whitesides GM. Spontaneous formation of ordered structures in thin films of metals supported on an elastomeric polymer. *Nature*, 1998, 393:146~149

45 Hutchinson JW and Suo Z. Mixed-mode cracking in layered materials. *Advances in Applied Mechanics*, 1991, 29:63~191

46 Reynolds O. On the theory of lubrication and its application to Mr. Beauchamp Tower's experiments, including an experimental determination of the viscosity of olive oil. Phil. Trans. Roy. Soc. London, 1886, **177**: 157~234

FIGURE CAPTIONS

Figure 1: Schematic of the fabrication process.

Figure 2: Part of a 100μm by 100μm island annealed for 90 minutes at 790ºC (Ref. 35).

Figure 3: A 200μm by 200μm island annealed for 90 minutes at 790ºC.

Figure 4: Schematic of the model.

Figure 5: Comparison between the shear lag model and the experiment data. (a) The average strain during anneal at 790°C. (b) The strain at the island center during anneal at 750°C (Ref. 35).

Figure 6: Schematic of the wrinkle growth rate as a function of the wrinkle wavelength.

Figure 7: Surface roughness as a function of anneal time. The dotted lines are from the linear perturbation analysis and the open symbols are from experiments (Ref. 35).

Figure 8: The wrinkle amplitude as a function of time for various islands sizes from numerical simulations (Ref. 34).

Figure 9: Schematic of the two-step anneal.

Figure 10: Large islands annealed with and without cap.

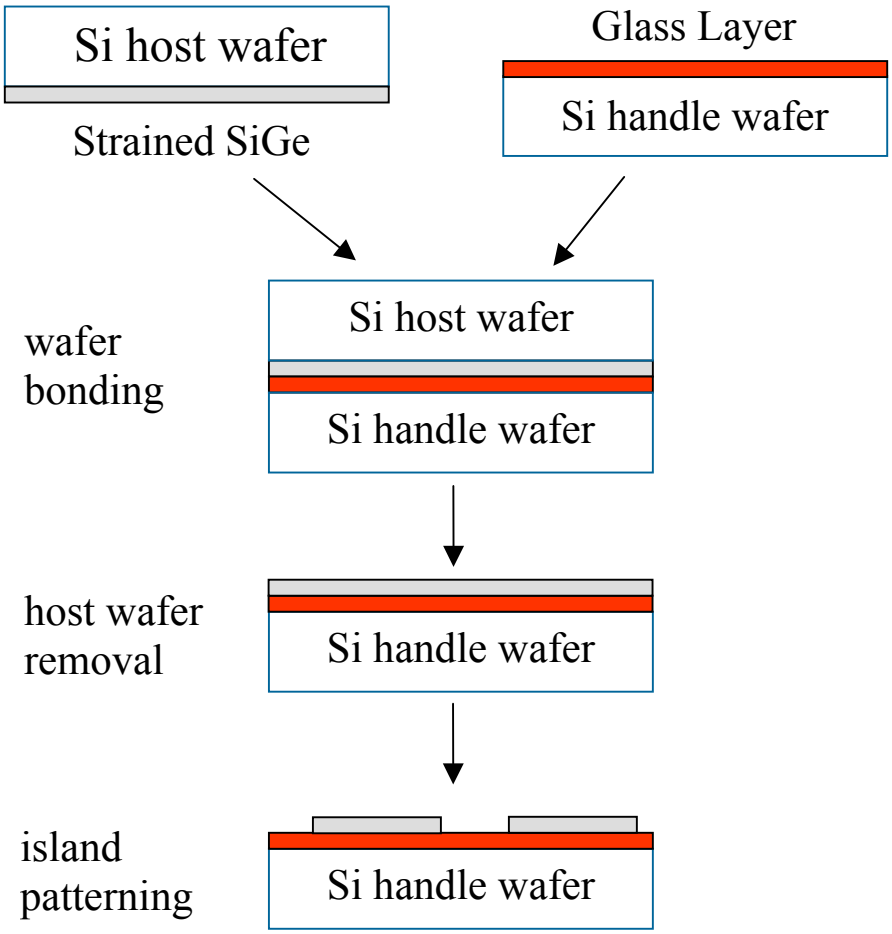
Si host wafer
Strained SiGe
Glass Layer
Si handle wafer
wafer bonding
Si host wafer
Si handle wafer
host wafer removal
Si handle wafer
island patterning
Si handle wafer

Figure 1

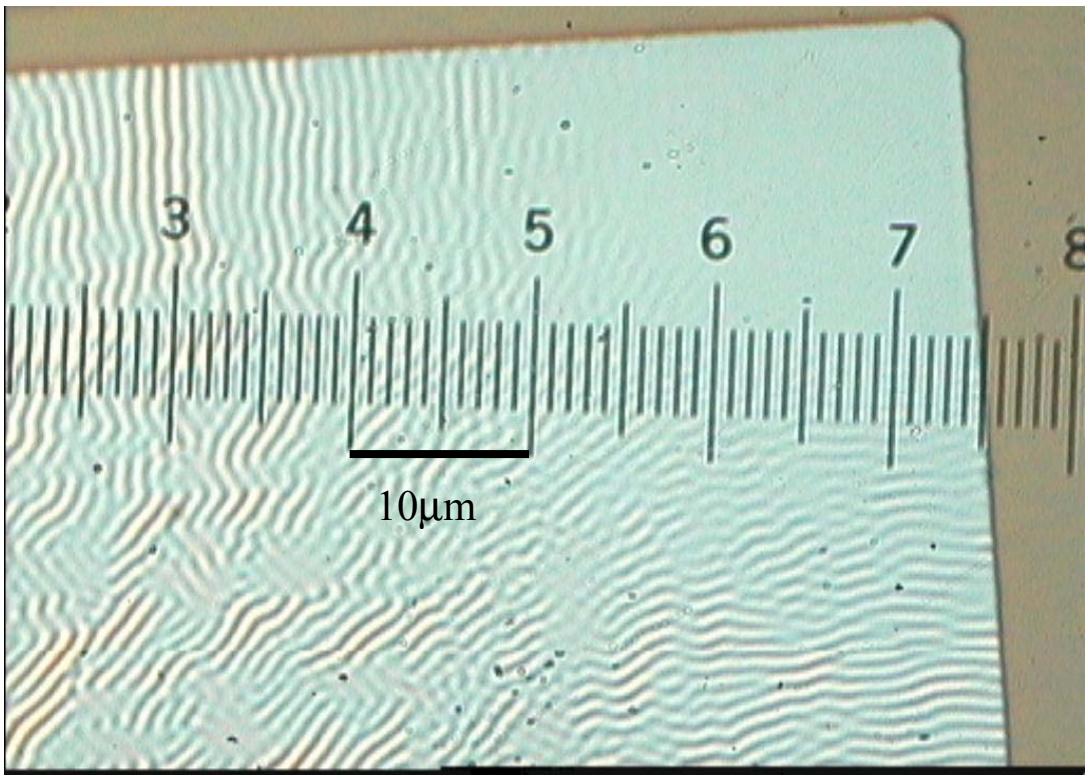

Figure 2

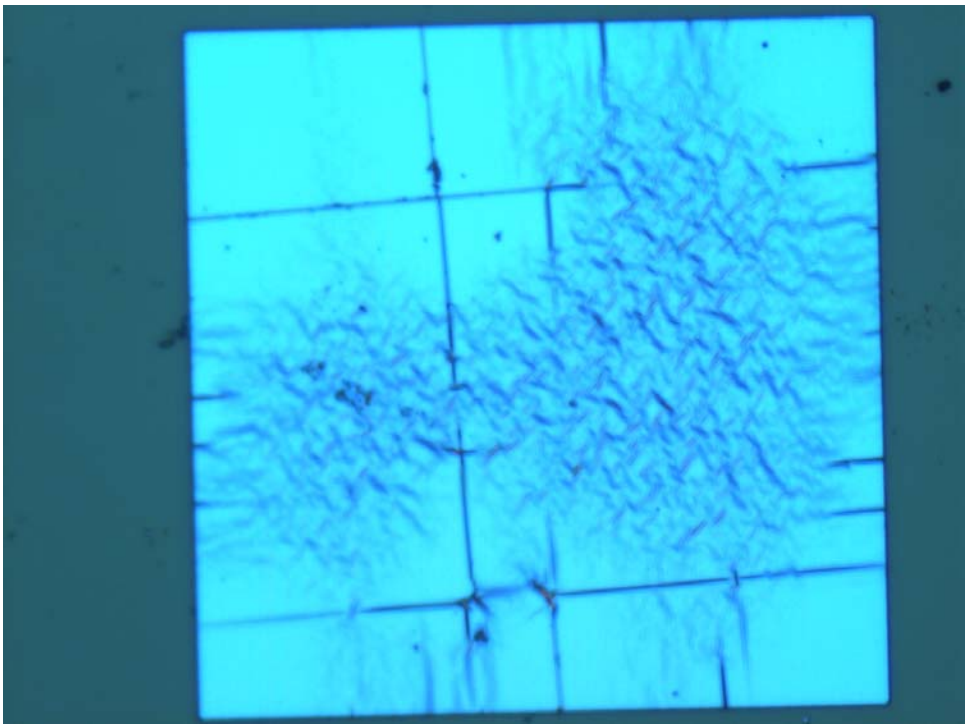

Figure 3

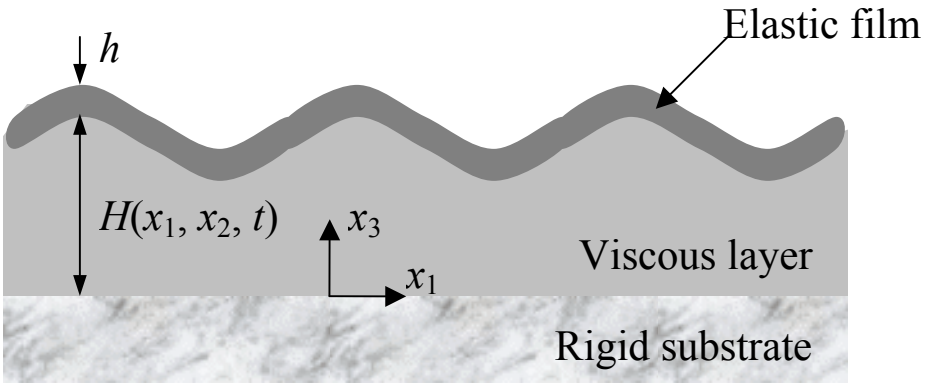

Figure 4

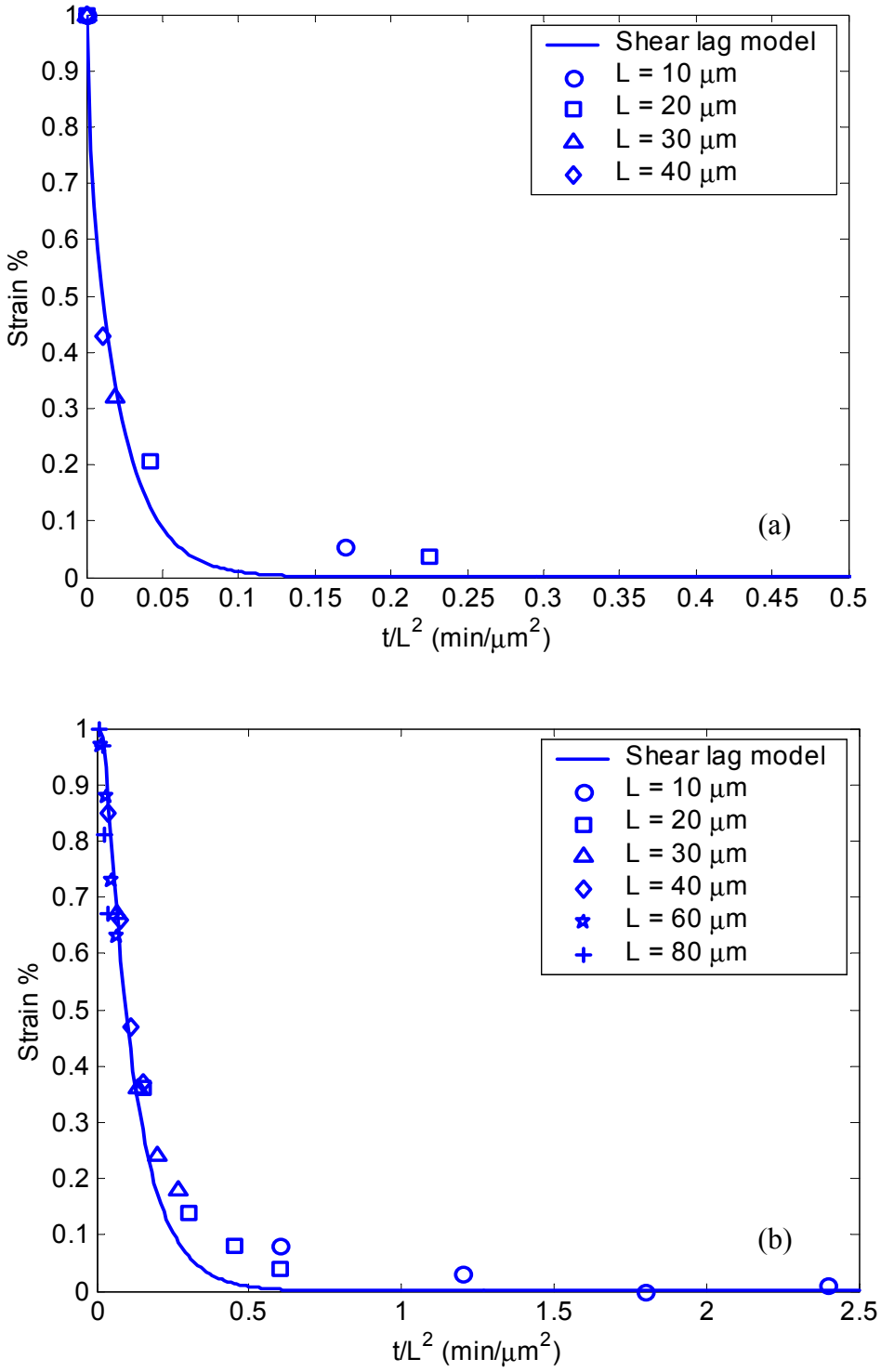
Shear lag model
L = 10 μm
L = 20 μm
L = 30 μm
L = 40 μm
L = 60 μm
L = 80 μm
Strain %
t/L2 (min/μm2)
(a)
(b)

Figure 5

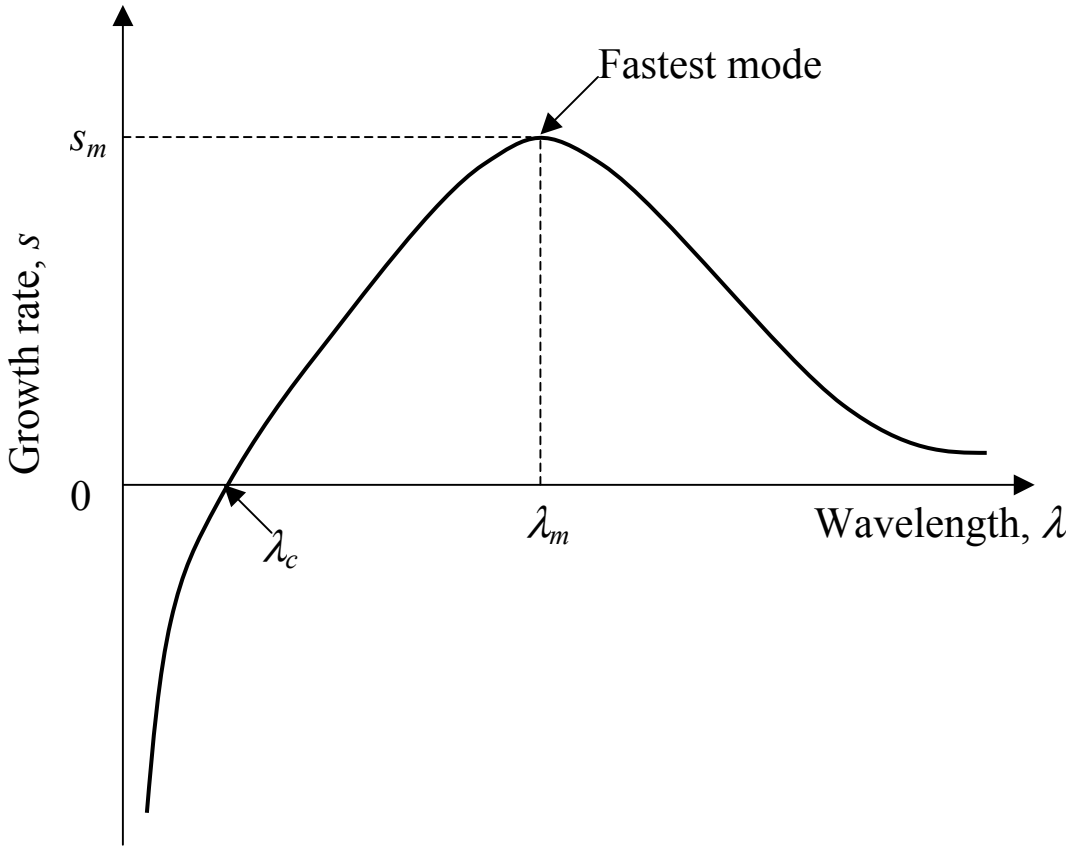
Fastest mode
s_m
Growth rate, s
0
λ_c
λ_m
Wavelength, λ

Figure 6

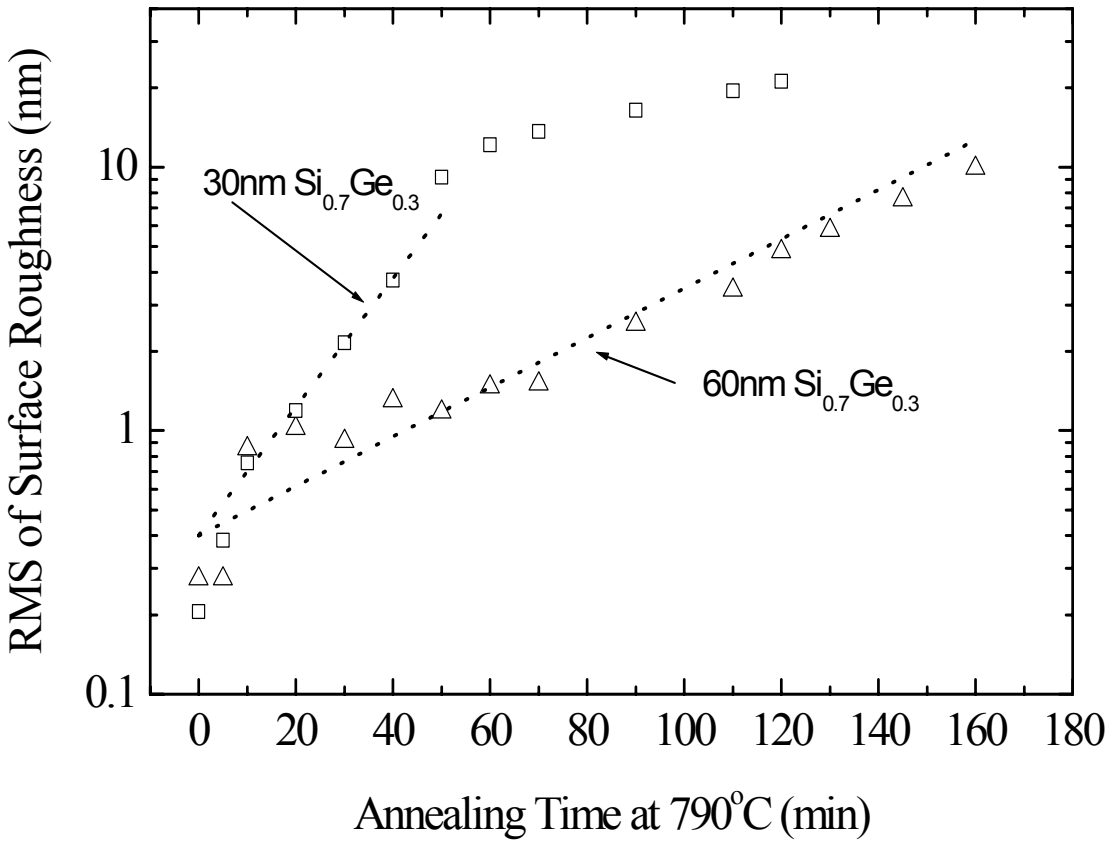
RMS of Surface Roughness (nm)
10
1
0.1
30nm Si0.7Ge0.3
60nm Si0.7Ge0.3
0
20
40
60
80
100
120
140
160
180
Annealing Time at 790°C (min)

Figure 7

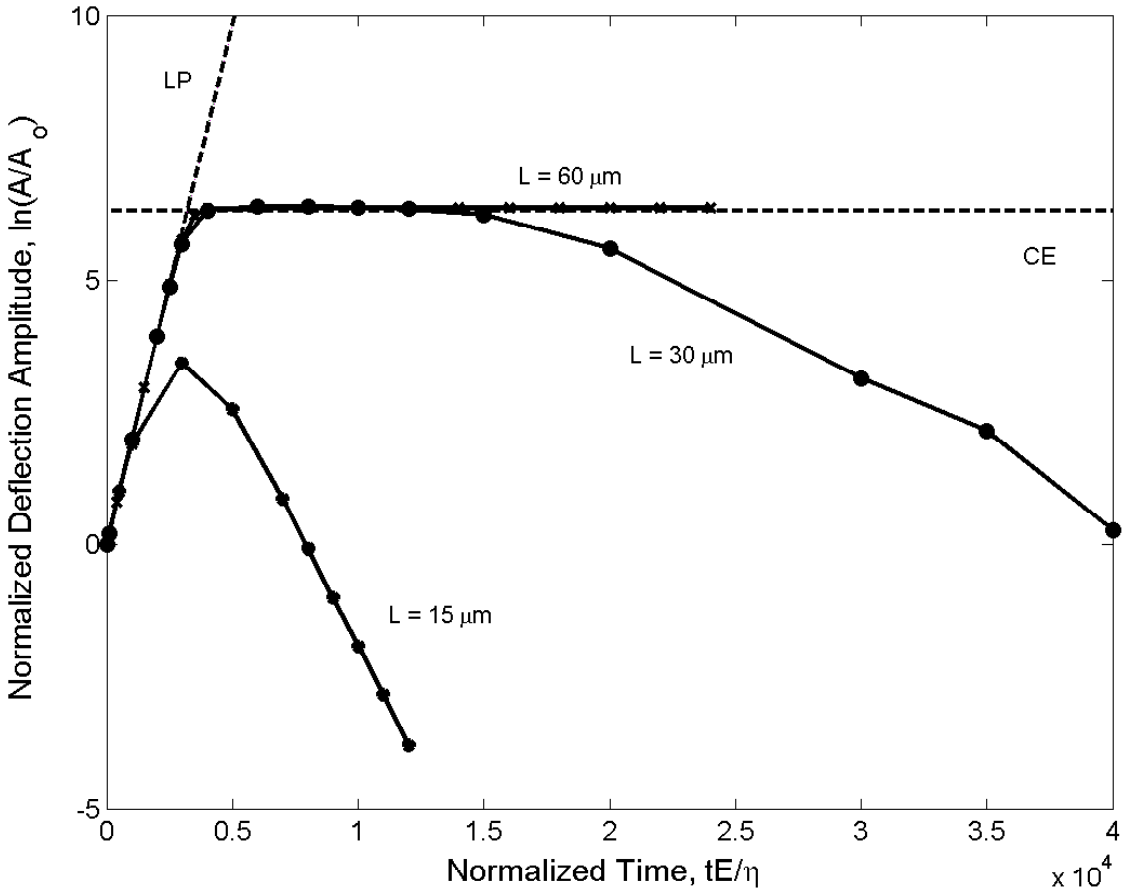
10
5
0
-5
0
0.5
1
1.5
2
2.5
3
3.5
4
x 10^4
Normalized Deflection Amplitude, ln(A/A_o)
Normalized Time, tE/η
LP
L = 60 μm
CE
L = 30 μm
L = 15 μm

Figure 8

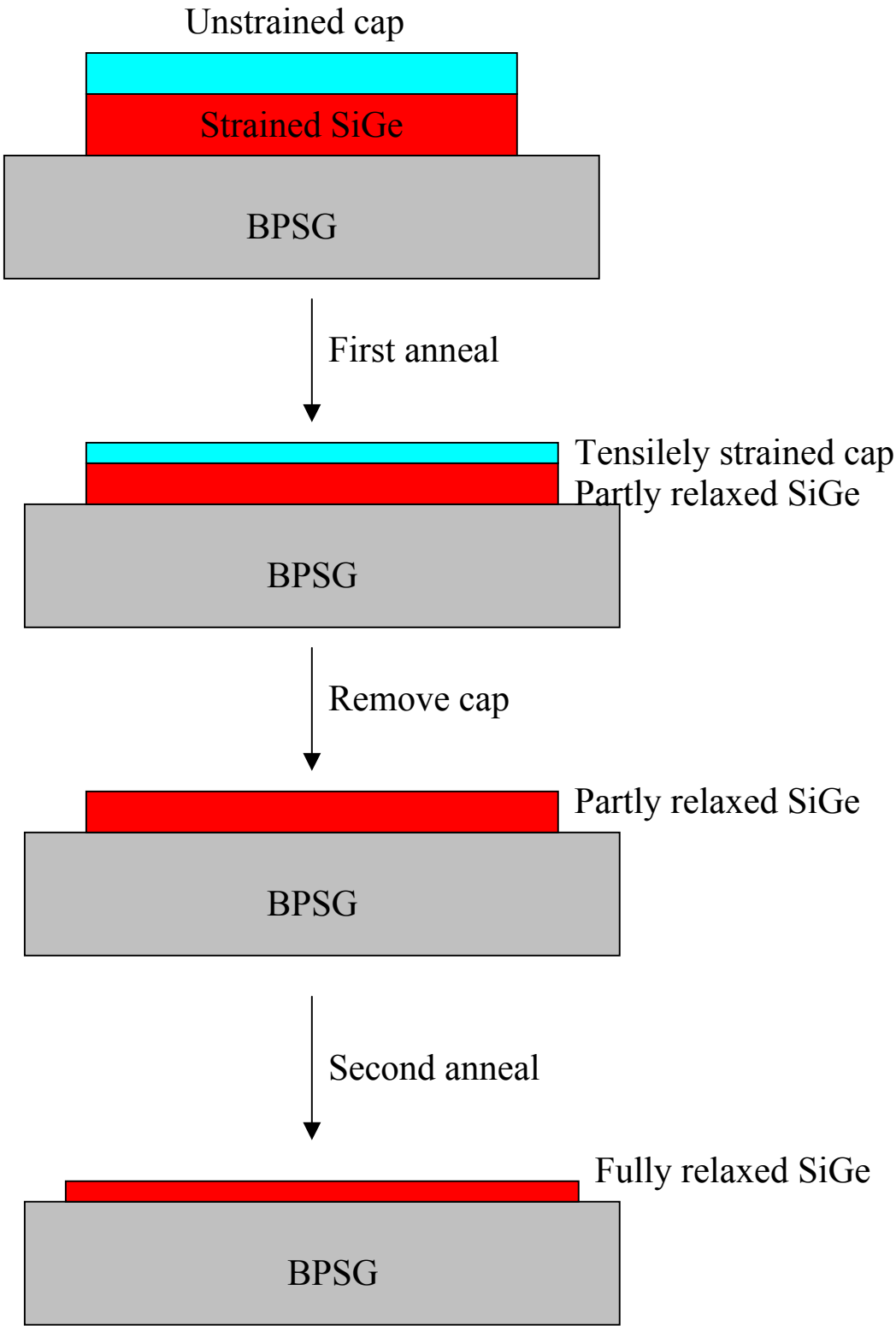
Unstrained cap
Strained SiGe
BPSG
First anneal
Tensilely strained cap
Partly relaxed SiGe
BPSG
Remove cap
Partly relaxed SiGe
BPSG
Second anneal
Fully relaxed SiGe
BPSG

Figure 9

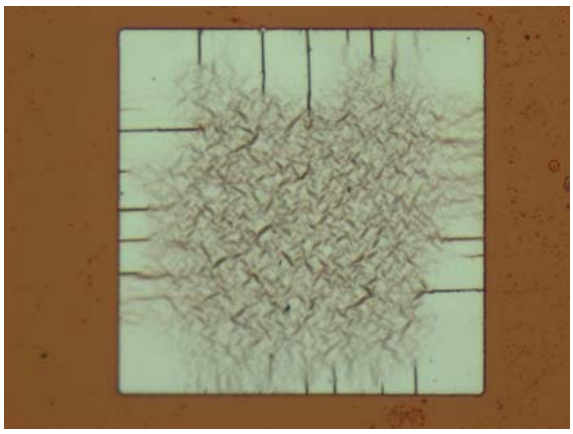

(a) L = 200µm, without cap

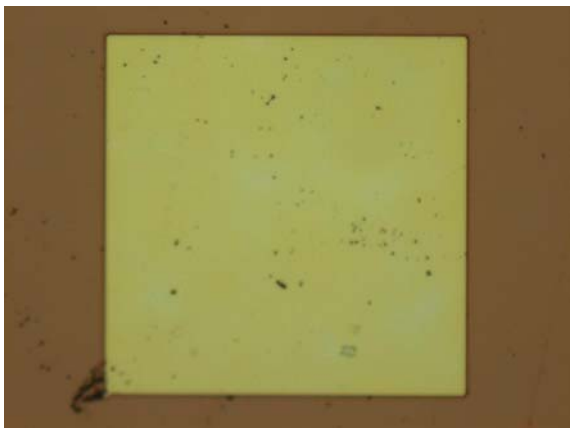

(b) L = 200µm, with a 19nm thick cap

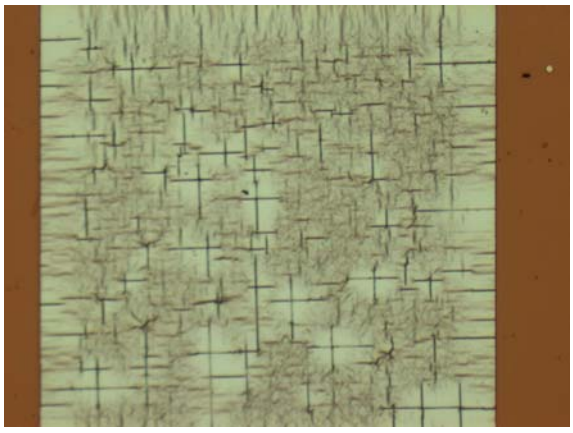

(c) L = 500µm, without cap

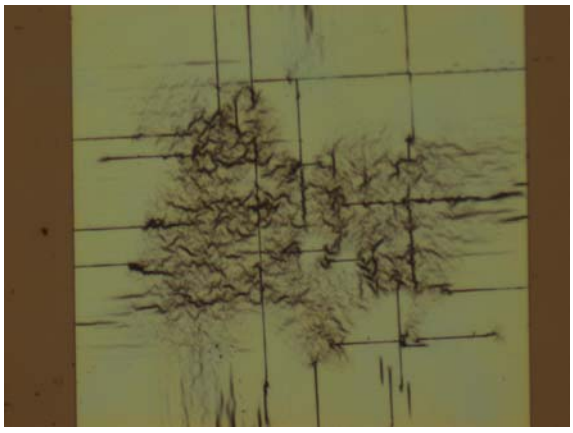

(d) L = 500µm, with a 19nm thick cap

Figure 10